

1 **Response to Referee #2:**

2 **General comment:**

3 *This work proposed a new method to estimate number concentrations of CCN based on the*
 4 *humidified nephelometer measurements. The advantages of this method are more convenient and*
 5 *cheaper than traditional measurements, and no other measurements are needed. The manuscript fits*
 6 *well to the scope of AMT. Thus I recommend it to be published after the following comments listed*
 7 *below have been adequately addressed.*

8 **Response:** Thanks for the comments. Comments are addressed point-by-point and corresponding
 9 responses are listed below.

10
 11 **Specific comments:**

12 1. *Lines 47-52: Please add some texts to evaluate each application. Also, I agree with another*
 13 *reviewer that one table should be added to summary the previous studies using aerosol optical*
 14 *properties to calculate NCCN.*

15 **Response:** Thanks for the suggestion. We have added descriptions and a table as follows:

16 “... Compared with the first kind, whose R^2 can be about 0.9, instruments used in the second kind
 17 of methods are cheaper and easier in operation, but has a lower accuracy of R^2 much lower than
 18 0.9. ...”

Campaign	Air mass	Parameter	Caveats	Results	Reference
ICARTT ¹ in the north eastern USA and Canada	Polluted air mass	fRH and PNSD	Calculate N_{CCN} with aerosol hygrosopicity contrained by f(RH) and PNSD.	Predict N_{CCN} at SS > 0.3% with a 0.9 R^2 .	Ervens et al., 2007
HaChi ² on the North China Plain	Aged continental air mass	PNSD and fRH	Similar to Ervens et al., 2007. Calculate N_{CCN} with the hygrosopicity parameter contrained by f(RH) and PNSD.	Slopes around 1 and R^2 around 0.9.	Chen et al., 2014
TARFOX ³ Atlantic seaboard and	Polluted air mass	Retrieved aerosol volume from	Predict N_{CCN} from aerosol volumes with empirical number-to-volume	Overestimate up to 5 times	Gasso and Hegg, 2003

ACE-2 ⁴		remote sensing	concentration ratio		
ACE-2 in northeastern Atlantic	Diverse air mass	Backscatter or extinction profile. CCN at the surface.	Retrieve N_{CCN} profile from backscatter (or extinction) vertical profile assuming their ratios are the same to the ratio at surface, which can be calculated by backscatter (or extinction) and N_{CCN} measured at the surface	Predict N_{CCN} on most days for 0.1% SS and on 20%–40% of the days at 1% SS.	Ghan and Collins, 2004
ARM ⁵ Climate Research Facility central site at the Southern Great Plains	Continental air mass	Backscatter (or extinction) and RH profile. fRH and CCN at surface	Same as Ghan and Collins, 2004.	Explains CCN variance for 25%–63% of all measurements at high supersaturations	Ghan et al., 2006
TRACE-P ⁶ and ACE-Asia ⁷	Asian outflow over the western Pacific	Aerosol Index (AI, the product of ambient light extinction and Å)	Predict N_{CCN} based on empirical relationship between AI and N_{CCN}	AI relate well to CCN only with suitably stratified data	Kapustin et al., 2006
Multiple measurements	Diverse air mass	AERONET aerosol optical thickness (AOT)	Predict N_{CCN} based on empirical relationship between AOT and N_{CCN} as a power law	Predict N_{CCN} at SS > 0.3% with a 0.88 R^2 , but have a factor-of-four range of N_{CCN} at a given AOT	Andreae, 2009
Four ARM sites	Polluted air mass	SSA, backscatter fraction and σ_{sp}	Estimate N_{CCN} from fitting parameters for the N_{CCN} activity spectra, which can be calculate based on their empirical relationships with aerosol optical properties.	Predict N_{CCN} with slopes around 0.9 and R^2 around 0.6.	Jefferson, 2010
Multiple ARM sites	Diverse air mass	RH, fRH, SSA, AOT	Calculate N_{CCN} with σ_{sp} (or AOT) based on their	Achieve the best results by using σ_{sp}	Liu and Li, 2014

around the world		and σ_{sp}	empirical relationship, whose impact RH, fRH and SSA.	and SSA. Weakly affect on the σ_{sp} - N_{CCN} relationship by fRH. Deteriorate N_{CCN} -AOT relationship with increasing RH	
Multiple ARM sites around the world	Diverse air mass not dominated by dust	\tilde{A} and extinction coefficient	Calculate N_{CCN} with light extinction based on their empirical relationship.	Deviate typically within a factor of 2.0.	Shinozuka et al., 2015

19 Tabel 1. Review of studies that have used aerosol optical parameters to infer N_{CCN} .

20 ¹ International Consortium for Atmospheric Research on Transport and Transformation.

21 ² Haze in China.

22 ³ Troposphere Aerosol Radiative Forcing Experiment.

23 ⁴ Second Aerosol Characterization Experiment.

24 ⁵ Atmospheric Radiation Measurement.

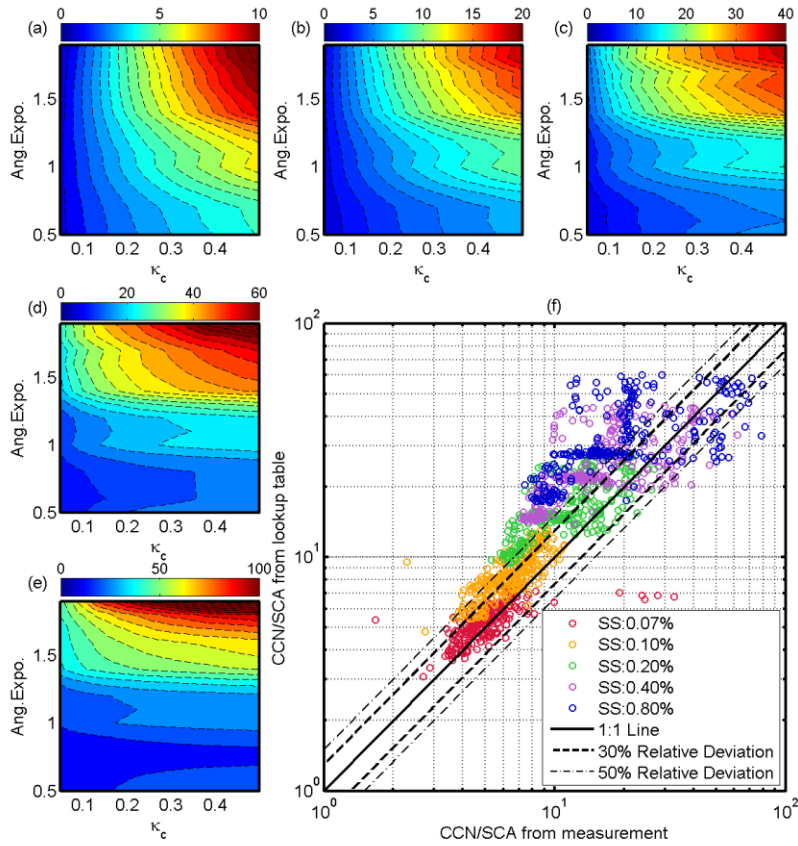
25 ⁶ Transport and Chemical Evolution over the Pacific.

26 ⁷ Aerosol Characterization Experiment-Asia.

27

28 2. Lines 172-176: I guess that the authors want to claim that the uncertainty will be smaller when
29 performing this method for shorter wavelength and lower supersaturation. Am I correct?
30 Concerning only one supersaturation (0.07%) was test in this study, and the relative deviation is
31 within 30%. Therefore, I am wondering that is it possible to perform this method to higher
32 supersaturations to check when the uncertainty will be larger than 50%.

33 **Response:** Thanks for the suggestion. Yes, the uncertainty is smaller when performing this
34 method for shorter wavelength and lower supersaturation. We apply this method to higher
35 supersaturations and compare calculated AR_{sp} with measured AR_{sp} . Δk at five supersaturations are
36 all set to be 0.2. Results are shown in Figure S2 as follows:



37

38 Figure S2. (a) to (e) Calculated AR_{sp} (ratios between N_{CCN} and σ_{sp} , represented as the color) based on σ_{sp} and
 39 N_{CCN} with different PNSDs classified by \tilde{A} and different κ_c at the five supersaturations. (f) Comparison between
 40 calculated AR_{sp} and measured AR_{sp} . Colors represent supersaturations.

41 As the lookup table at each supersaturation shown, calculated AR_{sp} is higher at higher
 42 supersaturation as a whole, which indicate more CCN with a common σ_{sp} . The same as shown in
 43 Figure 6, relative deviations of calculated AR_{sp} from measured AR_{sp} are generally within 30%.
 44 Calculated AR_{sp} at 0.10% supersaturation are 30% higher than measured AR_{sp} but still associated
 45 with measured AR_{sp} . For the three supersaturations higher than 0.10%, relative deviations of
 46 calculated AR_{sp} from measured AR_{sp} often exceed 50% and there is no significant correlation
 47 between calculated AR_{sp} and measured AR_{sp} . Results shown in Figure S2 verify the conclusion that
 48 the uncertainty is smaller when performing this method for shorter wavelength and lower
 49 supersaturation and the this method is not applicable at supersaturations higher than 0.10%.

50

51 3. Lines 180-181: How to calculate the differences (150 nm and 100 nm)? Please explain.

52 **Response:** Thanks for the suggestion. The diameter difference of cumulative contribution
 53 between 0.5 Å and 1.7 Å is roughly estimated by the average of differences where cumulative

contributions range from 0.2 to 0.8. We have revised the statement as: *“In detail, differences of cumulative contribution curves between 0.5 Å and 1.7 Å are about 150nm for σ_{sp} and about 100nm for N_{CCN} , by estimating the average of differences of diameters where cumulative contributions range from 0.2 to 0.8”*

4. *Line 191: What are smaller CCN-active particles? Do you mean Aitken mode particles? I think the contribution of particles smaller than 100 nm to σ_{sp} is always negligible.*

Response: Thanks for the comment. Smaller CCN-active particles refers to particles smaller than the average diameter of the whole CCN-active particles but is still CCN-active. For example, particles with diameters slightly larger than D_c contribute less to σ_{sp} than particles with diameters much larger than D_c . We have added the corresponding description after the sentence.

5. *Lines 201-203: See comment 2. It seems that you claim 0.07% is the highest supersaturation that can be applied for this method. Why? Do you have results for other supersaturations?*

Response: Thanks for the suggestion. Yes, as for the five supersaturations measured in this study, 0.07% is the highest supersaturation (also the only supersaturation) that can be applied for this method. This is because N_{CCN} at supersaturations higher than 0.07% are dominated by small particles more significantly than σ_{sp} (shown in Figure 1) and the correlation between N_{CCN} and σ_{sp} become weaker. The result in Figure S2 shows that relative deviations of calculated N_{CCN} at supersaturations higher than 0.07 can exceed 30% commonly.

6. *Lines 206-208: Add references. Why do you think κ_f is always lower than κ_c ? Any explanations?*

Response: Thanks for the suggestion. We have added reference as follows:

Irwin, M., N. Good, et al. (2010). "Reconciliation of measurements of hygroscopic growth and critical supersaturation of aerosol particles in central Germany." *Atmos. Chem. Phys.* 10(23): 11737-11752.

Good, N., D. O. Topping, et al. (2010). "Consistency between parameterisations of aerosol hygroscopicity and CCN activity during the RHaMBLe discovery cruise." *Atmospheric Chemistry and Physics* 10(7): 3189-3203.

Wex, H., M. D. Petters, et al. (2009). "Towards closing the gap between hygroscopic growth and activation for secondary organic aerosol: Part 1-Evidence from measurements." *Atmospheric*

85 *Chemistry and Physics* 9(12): 3987-3997.

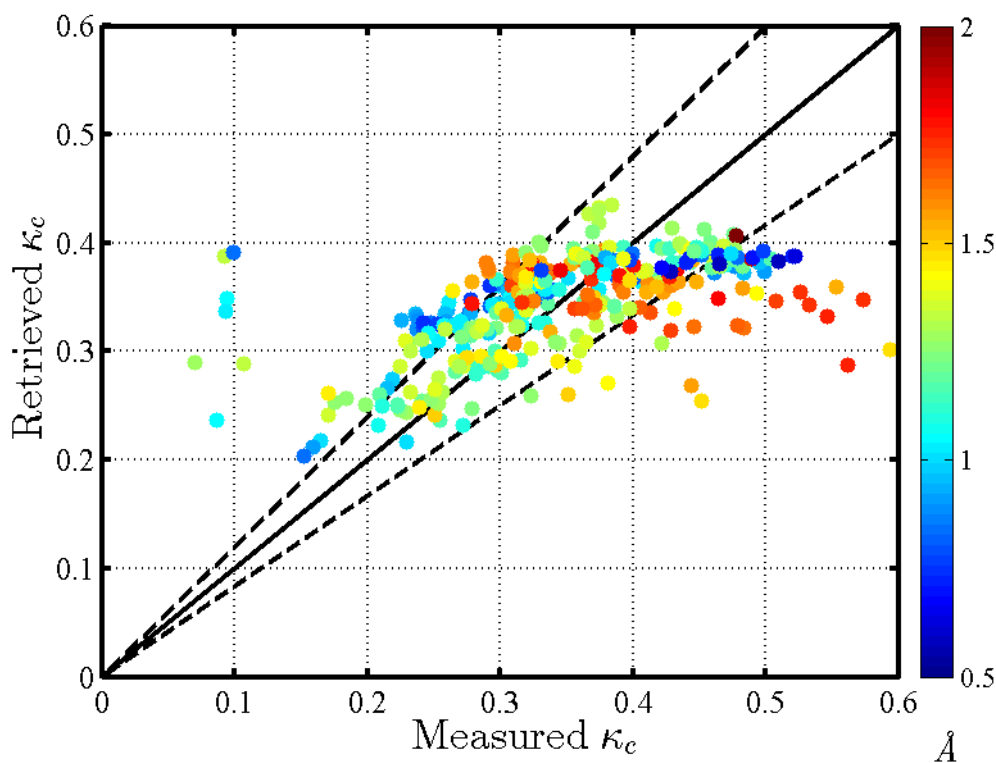
86 Renbaum-Wolff, L., M. Song, et al. (2016). "Observations and implications of liquid–liquid phase
87 separation at high relative humidities in secondary organic material produced by α -pinene
88 ozonolysis without inorganic salts." *Atmos. Chem. Phys.* 16(12): 7969-7979.

89 There are mainly two reasons why κ_f is always lower than κ_c . First, κ_f is calculated base on
90 measurments under subsaturated conditions while κ_c is calculated base on measurments under
91 supersaturated conditions. Studies found that aerosol hygroscopicity can increase under
92 supersaturated conditions, due to dissolution of slightly soluble substances (Wex et al., 2009), the
93 phase separation of organic compounds (Renbaum-Wolff et al., 2016) and so on. Second,
94 accumulation mode paticles are generally most hygroscopic. κ_f represent the average hygroscopicity
95 of total particles and is generally lower than hygroscopicities of accumulation mode paticles (Kuang
96 et al., 2017), while κ_c at 0.07% supersaturation indicate hygroscopicities of particles around 200nm.
97 As a result, κ_f is always lower than κ_c .

98

99 7. Lines 241-247 and Figure 5: How about the agreement between the retrieved and measured κ_c ?

100 **Response:** Thanks for the comment. We compare the retrieved and the measured κ_c , as shown in
101 Figure S3. For the majority of data points, relative deviations between retrieved and measured κ_c
102 are within about 20%. A large relative deviation much higher than 20% usually correspond to a \bar{A}
103 higher than 1.5, which is also shown in Figure 5.



104

Figure S3. Comparisons between measured and retrieved κ_c (dots) and their corresponding \dot{A} values (colors). The solid black line is the 1:1 line and dashed black lines indicate relative deviations of 20%.

8. *Lines 248-251: The authors claim that this method can only be adopted when \dot{A} is lower than 1.5. Is this conclusion only based on this study or can be used in different environments?*

Response: Thanks for the suggestion. This conclusion can be used in other environment, however the lookup table should be recalculated based on PNSD measured in corresponding environment.

9. *I suggest the authors reorganize or recheck the text for each figure caption. More information should be included, such as gray background in Figure 2 and black & dashed lines in Figure 6.*

Response: Thanks for the suggestion. There is no gray background in Figure 2 while gray backgrounds in Figure 4 are not described yet. We have revised them accordingly.

10. *Technical comments:*

Title: Nuclei.

Response: Thanks for the suggestion. We have revised it.

Line 36: also.

Response: Thanks for the suggestion.

Line 110: please provide DMA type.

Response: Thanks for the suggestion. It's Model 3081 DMA and we have revised it.

Lines 111 and 120: an electrostatic classifier.

Response: Thanks for the suggestion. We have revised them.

Line 126: campaigns. Line 133: there is no S in Eq. (1), please reformulate it.

Response: Thanks for the suggestion. It should be relative humidity (RH) and we have revised it.

Line 137: explain κ_f .

Response: Thanks for the suggestion.

Line 152: indicates.

134 **Response:** Thanks for the suggestion. We have revised it.

135 *Line 234: 0.5 to 1.5*

136 **Response:** Thanks for the suggestion. We have revised it.

137 *Lines 271-273: please add references.*

138 **Response:** Thanks for the suggestion.

139 *Line 308: changes*

140 **Response:** Thanks for the suggestion. We have revised it.

141 *There are still several grammar mistakes in the text, please carefully check.*

142 **Response:** Thanks for the suggestion.

143

144

145

Reference:

Wex, H., M. D. Petters, et al. (2009). "Towards closing the gap between hygroscopic growth and activation for secondary organic aerosol: Part 1-Evidence from measurements." *Atmospheric Chemistry and Physics* 9(12): 3987-3997.

Irwin, M., N. Good, et al. (2010). "Reconciliation of measurements of hygroscopic growth and critical supersaturation of aerosol particles in central Germany." *Atmos. Chem. Phys.* 10(23): 11737-11752.

Good, N., D. O. Topping, et al. (2010). "Consistency between parameterisations of aerosol hygroscopicity and CCN activity during the RHaMBLe discovery cruise." *Atmospheric Chemistry and Physics* 10(7): 3189-3203.

Renbaum-Wolff, L., M. Song, et al. (2016). "Observations and implications of liquid–liquid phase separation at high relative humidities in secondary organic material produced by α -pinene ozonolysis without inorganic salts." *Atmos. Chem. Phys.* 16(12): 7969-7979.

Kuang, Y., C. S. Zhao, et al. (2017). "A novel method for deriving the aerosol hygroscopicity parameter based only on measurements from a humidified nephelometer system." *Atmospheric Chemistry and Physics* 17(11): 6651-6662.

A New Method for Calculating Number Concentrations of Cloud Condensation ~~Nuclei~~ Nuclei Based on Measurements of A Three-wavelength Humidified Nephelometer System

Jiangchuan Tao¹, Chunsheng Zhao¹, Ye Kuang¹, Gang Zhao¹, Chuanyang Shen¹, Yingli Yu¹, Yuxuan Bian², Wanyun Xu²

[1]{Department of Atmospheric and Oceanic Sciences, School of Physics, Peking University, Beijing, China}

[2]{State Key Laboratory of Severe Weather, Chinese Academy of Meteorological Sciences}

*Correspondence to: C. S. Zhao (zcs@pku.edu.cn)

Abstract

The number concentration of cloud condensation nuclei (CCN) plays a fundamental role in cloud physics. Instrumentations of direct measurements of CCN number concentration (N_{CCN}) based on chamber technology are complex and costly, thus a simple way for measuring N_{CCN} is needed. In this study, a new method for N_{CCN} calculation based on measurements of a three-wavelength humidified nephelometer system is proposed. A three-wavelength humidified nephelometer system can measure aerosol light scattering coefficient (σ_{sp}) at three wavelengths and the light scattering enhancement factor (fRH). The Angstrom exponent (\AA) inferred from σ_{sp} at three wavelengths provides information on mean predominate aerosol size and hygroscopicity parameter (κ) can be calculated from the combination of fRH and \AA . Given this, a look-up table that involves σ_{sp} , κ and \AA is established to predict N_{CCN} . Due to the precondition for the application, this new method is not suitable for externally mixed particles, large particles (e.g. dust and sea salt) or particles near single source regions. This method is validated with direct measurements of N_{CCN} using a CCN counter on the North China Plain. Results show that relative deviations between calculated N_{CCN} and measured N_{CCN} are within 30% and confirm the robustness of this method. This method enables simpler N_{CCN} measurements because the humidified nephelometer system is easily operated and stable. Compared

with the method of CCN counter, another advantage of this newly proposed method is that it can obtain N_{CCN} at lower supersaturations in the ambient atmosphere.

1. Introduction

Cloud condensation nuclei (CCN) is the aerosol particle forming cloud droplet by hygroscopic growth. CCN number concentration (N_{CCN}) plays a fundamental role in cloud micro physics and aerosol indirect radiative effect. In general, the direct measurement of N_{CCN} is achieved in a cloud chamber under super-saturated conditions (Hudson, 1989;Nenes et al., 2001;Rose et al., 2008). Due to the requirement of high accuracies of working conditions like temperatures, vapors and flow rates in cloud chambers, the direct measurement of N_{CCN} is complex and costly (Rose et al., 2008;Lathem and Nenes, 2011). Thus, developments of simplified measurements of N_{CCN} are required. In recent years, attention has been focused on measurements of aerosol optical properties (Jefferson, 2010;Ervens et al., 2007;Gasso and Hegg, 2003), which are simple and well-developed (Covert et al., 1972;Titos et al., 2016). For aerosol population free of sea salt or dust, the accumulation mode aerosol not only dominates aerosol scattering ability but also contribute most to N_{CCN} . Thus, the calculation of N_{CCN} based on measurements of aerosol optical properties is feasible, and can facilitate N_{CCN} measurement.

There are two kinds of methods to calculating N_{CCN} based on measurements of aerosol optical properties. For the first kind, N_{CCN} as well as the hygroscopicity parameter (κ) can be calculated based on measurements of a humidified nephelometer system in combination with aerosol particle number size distribution (PNSD) (Ervens et al., 2007;Chen et al., 2014). Thus additional measurements of PNSD are needed. For the second kind, N_{CCN} is calculated based on statistical relationships between N_{CCN} and aerosol optical properties, such as scattering coefficient (σ_{sp}), Angstrom Exponent (\AA , which is the exponent commonly used to describe the dependence of σ_{sp} on wavelength) and single scattering albedo (SSA) (Jefferson, 2010;Shinozuka et al., 2015). Compared with the first kind, whose R^2 can be about 0.9, instruments used in the second kind of methods are cheaper and easier in operation, but has a lower accuracy of R^2 much lower than 0.9. Applications similar to the second kind are widely used in remote sensing. As shown in Table 1, Earlier-earlier

studies found that the aerosol volume or aerosol PNSD retrieved from remote sensing measurements can be used to calculate N_{CCN} (Gasso and Hegg, 2003; Kapustin et al., 2006). Recently, aerosol optical depth (AOD) or aerosol vertical profile is used to predict N_{CCN} directly (Ghan and Collins, 2004; Ghan et al., 2006; Andreae, 2009; Liu and Li, 2014).

In the statistical relationship between N_{CCN} and aerosol optical properties, σ_{sp} or AOD is mainly the proxy of aerosol absolute concentration, while \bar{A} or SSA can be used to reveal the variations of aerosol CCN activity, as shown in Table 1. Based on Kohler theory (Köhler, 1936; Petters and Kreidenweis, 2007), aerosol CCN activity is determined by aerosol size and aerosol chemical composition which is defined as aerosol hygroscopicity. Information about aerosol size and aerosol hygroscopicity are critical to N_{CCN} prediction and their absence can lead to a deviation with factor of four (Andreae, 2009). Compared with aerosol hygroscopicity, aerosol size is more important in determining CCN activity (Dusek et al., 2006). The value of \bar{A} can provide information on mean predominate aerosol size (Brock et al., 2016; Kuang et al., 2017a). As a result, N_{CCN} calculation from \bar{A} and extinction coefficient is found to be accurate to some extent (Shinozuka et al., 2015). As proxies for aerosol hygroscopicity, SSA or aerosol light scattering enhancement factor (fRH) is commonly used while not so effective (Jefferson, 2010; Liu and Li, 2014). SSA is determined by the ratio between the light absorbing carbonaceous and less-absorbing components. Black carbon dominates the absorption of solar radiation and is a main hydrophobic composition as well. Black carbon contributes most to the light absorbing carbonaceous and is the most important hydrophobic compositions as well. Less-absorbing components consist of inorganic salts and acids, as well as most organic compounds, which are generally hygroscopic compositions. SSA correlates positively with aerosol hygroscopicity (Rose et al., 2010) but deviates significantly due to the diversity of hygroscopicity of less-absorbing components. Thus N_{CCN} calculation combining SSA, backscatter fraction and σ_{sp} still lead to significant deviations, with a 0.6 R^2 (Jefferson, 2010). Thus deviations of N_{CCN} calculation based on SSA is of large errors (Jefferson, 2010). As for fRH, there was a study applied aerosol optical quantities (σ_{sp} or aerosol optical thickness) with fRH or SSA to calculate N_{CCN} (Liu and Li, 2014). In their study, compared with the combination of SSA and aerosol optical quantities, the combination of fRH and aerosol optical quantities is found to be less effective in

~~estimating N_{CCN} , even though fRH directly connected with aerosol hygroscopicity (Liu and Li, 2014).~~
~~Compared with SSA, previous studies found fRH to be less effective in estimating N_{CCN} , even~~
~~though fRH directly connected with aerosol hygroscopicity (Liu and Li, 2014).~~ This may result from
the significant dependence of fRH on aerosol size (Chen et al., 2014; Kreidenweis and Asa-Awuku,
2014; Kuang et al., 2017a). As mentioned before, PNSD is used for better calculation of κ and N_{CCN}
from fRH in previous studies (Ervens et al., 2007; Chen et al., 2014). A new method to estimate κ
from fRH and \bar{A} was proposed recently (Kuang et al., 2017a; Brock et al., 2016). Based on this
method, fRH can be used to calculate N_{CCN} without measurements of PNSD and can be expected to
improve the N_{CCN} prediction just based on measurements of aerosol optical properties.

In this study, the relationship between N_{CCN} and aerosol optical properties measured by a
humidified nephelometer system is studied and a new method for N_{CCN} prediction is proposed. This
new method is validated based on data observed in Gucheng campaign on the North China Plain and
can be expected to improve measurements of N_{CCN} due to advantages of applying nephelometers.

2. Methodology

2.1. Data

Data in this study are mainly measured at Gucheng (39.15N, 115.74E) during autumn in 2016
on the North China Plain (NCP). Gucheng is 100km southwest from Beijing and 40km northeast
from Baoding under background pollution condition in the NCP. The observation site was
surrounded by farmland and about 3km away from the Gucheng town. This campaign started on 20
October and lasted for nearly one month.

Instruments used in Gucheng campaign were located in a measurement container under
temperature maintained at 25 °C. Ambient aerosol was sampled and dried to relative humidity (RH)
lower than 30% by an inlet system consisting of a PM10 inlet, an inline Nafion dryers and a RH and
temperature sensor (Vaisala HMP110). Then the sample aerosol was separated by a splitter and
directed into various instruments. During this campaign, aerosol scattering coefficient (σ_{sp}), aerosol
optical hygroscopic growth factor (fRH), particle size-resolved activation ratio (AR) and particle
number size distribution (PNSD) were obtained.

fRH as well as σ_{sp} at three wavelengths were measured by a humidified nephelometer system consisting of two nephelometers (Aurora 3000, Ecotech Inc.) and a humidifier. σ_{sp} can be described by a formula of Å:

$$\sigma_{sp}(\lambda) = \beta \cdot \lambda^{-\text{Å}}, \quad (1)$$

where β is the aerosol number concentration and λ is the wavelength. Thus Å can be calculated directly from σ_{sp} measured by a nephelometer. The humidifier with a Gore-Tex tube humidified the sample air up to 90% RH. A whole cycle of humidification lasted about 45 minutes from 50% RH to 90% RH. Dried σ_{sp} was obtained directly from dried sample aerosol measured by one nephelometer and humidified σ_{sp} was obtained from humidified aerosol measured by another nephelometer.

~~fRH/RH~~ is defined as:

$$fRH = \sigma_{sp}(RH) / \sigma_{sp} \quad (2)$$

~~where $\sigma_{sp}(RH)$ is the humidified σ_{sp} at each RH, the ratio of the humidified σ_{sp} to the dried σ_{sp} at each RH.~~ Detailed description of the humidified nephelometer system was illustrated in Kuang et al (2017a).

The particle size-resolved activation ratio (AR), defined as the ratio of N_{CCN} to total particles, was measured by a system mainly consisting of a differential mobility analyzer (DMA, Model 3081) and a continuous-flow CCN counter (model CCN200, Droplet Measurement Technologies, USA; Roberts and Nenes (2005); Lance et al., (2006)). The system selected mono-disperse particles with the DMA coupled with an electrostatic classifier (model 3080; TSI, Inc., Shoreview, MN USA) and measured AR of the mono-disperse particles by a condensation particle counter (CPC model 3776; TSI, Inc.) and CCN counter. Ranges of particle size and supersaturation were 10-300nm and 0.07%-0.80%, respectively. Measurements at five supersaturations (0.07%, 0.10%, 0.20%, 0.40% and 0.80%) were conducted sequentially ~~and with~~ each cycle lasted for 1 hour, and N_{CCN} at 0.07% supersaturation was used in this study. Before and after the campaign, supersaturations set in this system were calibrated using ammonium sulfate (Rose et al., 2008). More information about the system are given in Deng et al. (2011) and Ma et al. (2016).

PNSD with particle diameter from 9nm to 10um was measured by a mobility particle size

spectrometer (SMPS, TSI Inc., Model 3996) and an Aerodynamic Particle Sizer (APS, TSI Inc., Model 3321). SMPS consisted of a DMA, an electrostatic classifier and a CPC (model 3776; TSI, Inc., Shoreview, MN USA) and measured PNSD with diameter lower than 700nm.

In addition, PNSD and σ_{sp} from 2011 to 2014 at four campaigns (Wuqing in 2011, Xianghe in 2012 and 2013, and Wangdu in 2014) in NCP were used in this study. PNSD in these campaigns was measured by a Twin Differential Mobility Particle Sizer (TDMPS, Leibniz-Institute for Tropospheric Research (IfT), Germany) and an Aerodynamic Particle Sizer (APS, TSI Inc., Model 3321). A TSI 3563 nephelometer was used to obtain σ_{sp} at three wavelengths. Details about the four campaigns can be found in Ma et al. (2011), Ma et al.(2016), Kuang et al. (2016) and Kuang et al.(2017a).

2.2. Theories

Hygroscopic growth of particles at certain relative humidity can be described by κ -Köhler theory (Petters and Kreidenweis, 2007):

$$\frac{RH}{100} = \frac{g(RH)^3 - 1}{g(RH)^3 - (1 - \kappa)} \cdot \exp\left(\frac{4\sigma_{s/a} \cdot M_w}{R \cdot T \cdot D_d \cdot g \cdot \rho_w}\right) \quad (1)$$

where $g(RH)$ is geometric diameter growth factor, κ is the hygroscopicity parameter, $S-RH$ is the ~~saturation ratio~~ relative humidity; ρ_w is the density of water; M_w is the molecular weight of water; $\sigma_{s/a}$ is the surface tension of the solution–air interface, which is assumed to be equal to the surface tension of the pure water–air interface; R is the universal gas constant; and T is the temperature.

Accounting for the impact of \tilde{A} , κ_f can be derived directly from fRH (Brock et al., 2016;Kuang et al., 2017a). A single-parameter parameterization scheme proposed by Brock et al. (2016) connects fRH and κ by the approximately proportional relationship between total aerosol volume and σ_{sp} :

$$f(RH) = 1 + \kappa_{sca} \cdot RH / (100 - RH) \quad (2)$$

where κ_{sca} is a parameter for fitting fRH curves and is found can be used to predict κ_f in combination with \tilde{A} in recent studies (Brock et al., 2016;Kuang et al., 2017a).~~can determines κ_f with \tilde{A} . This method of calculating κ_f based on κ_{sca} and \tilde{A} was confirmed by good agreement with κ_f calculated from fRH and PNSD. This method was confirmed by good agreement with κ_f~~

~~calculated from $f(RH)$ and $g(RH)$~~ (Brock et al., 2016; Kuang et al., 2017a).—

N_{CCN} can be calculated from size-resolved AR at a certain supersaturation (SS) and PNSD (referred to as $n(\log D_p)$) as follows:

$$N_{CCN} = \int_{\log D_p} AR(\log D_p, SS) \cdot n(\log D_p) d \log D_p \quad (3)$$

In general, size-resolved AR curves are complicated and always replaced by a critical diameter to simplify calculation (Deng et al., 2013). The critical diameter is defined as:

$$N_{CCN} = \int_{\log D_c}^{\log D_{p,max}} n(\log D_p) d \log D_p \quad (4)$$

where $D_{p,max}$ is the maximum diameter of the measured particle number size distribution. In other words, the integral of PNSD larger than D_c equals to the measured N_{CCN} . And a critical κ (κ_c) can be calculated by equation (1) and ~~indicated-indicates~~ CCN activity and hygroscopicity of particles.

3. Results

3.1. Calculation of N_{CCN} based on measurements of a Humidified Nephelometer system

Free of sea salt aerosol and dust aerosol, accumulation mode aerosol dominates both the optical scattering ability at short wavelengths and the CCN activity at low supersaturations, and thus a reasonable relationship between σ_{sp} and N_{CCN} can be achieved. Figure 1 shows the size distribution of cumulative contributions of σ_{sp} at 450nm and N_{CCN} at 0.07% with various \AA and κ_c , and corresponding normalized PNSDs based on data measured at the four campaigns on the North China Plain. During the four campaigns, no sea salt aerosol or dust aerosol was observed (Ma et al., 2011; Ma et al., 2016; Kuang et al., 2016; Kuang et al., 2017a). For continental aerosol without sea salt or dust, \AA varies from 0.5 to 1.8 and κ_c varies from 0.1 to 0.5 (Cheng et al., 2008; Ma et al., 2011; Liu et al., 2014; Kuang et al., 2017b). And as mentioned before, \AA can be used as a proxy of the overall size distribution of aerosol populations, with smaller \AA indicating more larger particles. In figure 1, comparisons for \AA are made between 0.5 and 1.71.9 and for κ_c are made between 0.1 and 0.5. As larger particles contribute more to light scattering and activation, cumulative

contributions of both σ_{sp} and N_{CCN} increase significantly at the diameter range of accumulation mode particles. Because more hygroscopic particles are able to activate at smaller diameters, the cumulative contribution of N_{CCN} with higher κ_c increases at smaller diameters. In general, major contributions of both σ_{sp} and N_{CCN} are made by particles from 200nm to 500nm for various \bar{A} and κ_c . This implies the feasibility of inferring N_{CCN} from aerosol optical properties.

~~Because particles smaller than 200nm can activate at supersaturations higher than 0.07% while scatter less light at wavelengths longer than 450nm, which are shown as the light color lines in Figure 1. Because smaller particles can activate at higher supersaturations while scatter less light at longer wavelengths,~~ it's obvious that significant differences will exist between cumulative contributions of σ_{sp} and N_{CCN} . This means σ_{sp} and N_{CCN} are dominated by different particles and poor correlation between σ_{sp} and N_{CCN} can be expected. Thus the method of inferring N_{CCN} from aerosol optical properties is applicable for shorter wavelength and lower supersaturations.

Furthermore, PNSD with higher \bar{A} indicates ~~as~~ more Aitken mode particles and fewer accumulation mode particles. Thus large particles contribute less for both σ_{sp} and N_{CCN} when \bar{A} are higher, characterizing an increase of cumulative contribution curves at smaller diameters. In detail, ~~differences of cumulative contribution curves between 0.5 \bar{A} and 1.9 \bar{A} are about 150nm for σ_{sp} and about 100nm for N_{CCN} , by estimating the average of differences of diameters where cumulative contributions range from 0.2 to 0.8. differences between cumulative contribution curves with \bar{A} of 0.5 and 1.7 are about 150nm and 100nm for σ_{sp} and N_{CCN} , respectively.~~ Changes of cumulative contributions of N_{CCN} and σ_{sp} with various \bar{A} reveal that the shape of PNSD can influence the correlation between N_{CCN} and σ_{sp} . This is confirmed by previous studies in which the \bar{A} is found to play an important role in calculating N_{CCN} from σ_{sp} (Shinozuka et al., 2015; Liu and Li, 2014).

The relationship between σ_{sp} and N_{CCN} dependent on \bar{A} and κ_c is evaluated by calculating σ_{sp} and N_{CCN} with different PNSDs (classified by \bar{A}) and different κ_c . In detail, ratios of N_{CCN} to

σ_{sp} , referred to as AR_{sp} , are calculated to eliminate the effect of variations of particle concentrations consistent at all diameters. Results at the supersaturation of 0.07% are shown in figure 2 and AR_{sp} is higher than 0 and lower than 10 range from 0 to 10. In general, AR_{sp} are higher for more hygroscopic particles or smaller particles. As particles become more hygroscopic, more CCN can be expected when σ_{sp} is fixed. As aerosol populations consist of more smaller CCN-active particles, the increase of σ_{sp} is weaker than that of N_{CCN} . For example, particles with diameters slightly larger than D_c contribute less to σ_{sp} than particles with diameters much larger than D_c .

In detail, the sensitivity of AR_{sp} to \tilde{A} also changes with \tilde{A} and κ_c . When \tilde{A} are higher than 1.4 and κ_c is lower than 0.2, AR_{sp} is insensitive to \tilde{A} . While when \tilde{A} are lower than 1 and κ_c are higher than about 0.3, AR_{sp} is more sensitive to \tilde{A} than κ_c . Higher-This higher sensitivity of AR_{sp} to \tilde{A} are found with higher κ_c and lower \tilde{A} , which reveals that particles having mean predominate size smaller more small particles and less large particles than existing particles can contribute more to N_{CCN} . This is the consequence of the sensitivity of AR_{sp} to \tilde{A} resulting from the variation of small CCN-active particles, as mentioned before.

Based on the lookup-table illustrated in Figure 2, N_{CCN} at the supersaturation of 0.07% can be calculated simply from \tilde{A} , κ_f and σ_{sp} which can be obtained from measurements of a humidified nephelometer system. The description of this simple method is shown in figure 3. A new look-up table needs to be made for N_{CCN} estimation at other supersaturations, which should better be less than 0.07% as mentioned in the discussion of figure 1.

One critical issue about the method is the conversion of the κ_f obtained from the humidified nephelometer system to the κ_c under super-saturated conditions. There are mainly two factors making this conversion necessary. First, closure studies of aerosol hygroscopicity found significant deviations between hygroscopicity at sub-saturated conditions and super-saturated conditions (Wex et al., 2009; Irwin et al., 2010; Good et al., 2010; Renbaum-Wolff et al. 2016). Their difference can be expected to be about 0.1 for accumulation mode aerosol (Wu et al., 2013; Whitehead et al., 2014; Ma et al., 2016). Second, the κ_f indicates the hygroscopicity of total particles and can be quite different from aerosol hygroscopicity at a specific diameter due to variations of size distributions

~~of size-dependent~~ particle hygroscopicity. Kuang et al. (2017a) found a difference around 0.1 between κ_f and κ_c inferred from g(RH) measurements for accumulation mode particles whose κ_f is no larger than 0.2. In this study, a simple conversion that κ_c is 0.2 higher than κ_f is used to calculate N_{CCN} , while for κ_f larger than 0.2, a smaller difference of 0.1 between κ_c and κ_f should be used (Kuang et al., 2017a). This simplified relationship between κ_c and κ_f is a rough estimate regardless of the complexity of differences of aerosol hygroscopicity measured by different instruments, but still used in this study for two reasons~~is applicable for two reasons. On one hand~~First, the accurate conversion cannot be achieved without detailed information of the particle hygroscopicity, which is difficult and complicated to measure. ~~On the other hand~~Second, a deviation of κ_c less than 0.1 generally leads to a deviation of N_{CCN} less than 20% (Ma et al., 2016), which is comparable with the deviation of CCN measurements. As a result, for a simple method of N_{CCN} calculation, this conversion is quite easy~~and adequate enough~~. In addition, it is important to note that the value of the difference between κ_c and κ_f is also a rough estimate regardless of the complexity of aerosol hygroscopicity under different conditions, and the influence of $\Delta\kappa$ deviation on N_{CCN} calculation needs to be further examined based on field observation. In regions of single aerosol emissions or productions, the actual $\Delta\kappa$ can be too large (some organic compositions, Wex et al., 2009; Renbaum-Wolff et al., 2016) or too small (inorganic compositions and black carbon) and thus is not suitable for the application of this method.

Besides aerosol size and hygroscopicity, aerosol mixing state can also affect aerosol cloud activity. When primary aerosol emissions are strong, aerosol populations are likely to be externally mixed and a realistic treatment of aerosol mixing state is critical for N_{CCN} calculation (Cubison et al., 2008; Wex et al., 2010). But for regions away from strong aerosol primary emissions, the influence of mixing state on aerosol cloud activity is small and the assumption of internal mixing state is effective for the estimation of N_{CCN} (Dusek et al., 2006; Deng et al., 2013; Ervens et al., 2010). For regions above the boundary layer where clouds form and measurements of N_{CCN} are important, this conclusion is tenable if there are no plumes (Moteiki and Kondo, 2007; McMeeking et al., 2011). In the new method of this paper aerosol populations are assumed to be internally mixed. Thus this method might not be applicable for regions or air masses greatly affected by strong primary aerosol emissions. Furthermore, this new method cannot be applied for regions where sea salt or dust prevails, as mentioned before. In summary, this method can be used to calculate N_{CCN} for continental

regions, especially at clouds forming heights, where aged aerosol particles dominate.

3.2. Validation based on N_{CCN} measurement

The method for calculating N_{CCN} based on measurement of the humidified nephelometer system, including the conversion of κ_c and the lookup-table, is examined using data measured in Gucheng.

Overview of data in Gucheng is shown in Figure 4. From polluted periods to clean periods, significant variations of N_{CCN} and σ_{sp} can be found but AR_{sp} of N_{CCN} to σ_{sp} stays around 5. On October 23rd and 29th, N_{CCN} and σ_{sp} are lower than 2000#/cm³ and 500Mm⁻¹, respectively. While on October 20th, 26th and November 3rd, N_{CCN} and σ_{sp} are higher than 2000#/cm³ and 500Mm⁻¹, respectively. These variations of N_{CCN} and σ_{sp} are mainly due to the variation of the particle number concentration rather than ~~the shape of particle size distribution and aerosol hygroscopicity~~~~the particle microphysical properties~~. Variations of AR_{sp} result from the variations of \tilde{A} and κ_c , which indicate the variations of aerosol microphysical properties and chemical compositions.

In general, AR_{sp} is more sensitive to variations of \tilde{A} than κ_c . As mentioned before, the sensitivity of AR_{sp} to \tilde{A} is determined by both \tilde{A} and κ_f . In detail, \tilde{A} during the campaign mainly ranges from 0.5 to ~~1.5~~1.5 and κ_f ranges mainly from 0.05 to 0.2, which means that κ_c ranges from 0.25 to 0.4. These values of \tilde{A} and κ_f correspond a significant sensitivity of AR_{sp} to \tilde{A} , as the lookup table shows in figure 2. The sensitivity of AR_{sp} to κ_c is much small and only notable during some short periods (grey bars in Figure 4). For example, from November 5th to 7th, variations of κ_f and \tilde{A} are opposite and result in nearly constant AR_{sp} . And from October 30th to November 2nd, consistent variations of \tilde{A} and κ_f lead to greater variations of AR_{sp} than other periods. This weak sensitivity of AR_{sp} to κ_f may be due to the uncertainty of κ_c calculated from κ_f based on the simplified conversion.

This simplified conversion of κ_c is examined by comparing κ_f and κ_c measured in Gucheng campaign, shown in Figure 5. In general, $\Delta\kappa$ that indicates the difference between κ_f and κ_c is around 0.2 and independent from \tilde{A} and κ_c . Over 80% of $\Delta\kappa$ ranges from 0.1 to 0.3 that confirms applicability of the simplified conversion of κ_c . However, a notable deviation of $\Delta\kappa$ can be found when \tilde{A} is higher than 1.5. High values of \tilde{A} represent existence of small particles. Compositions

and mixing state of these small particles, which may be fresh emitted and experience inefficient aging processes, are diverse and likely to deviate from the simplified conversion of κ_c .

Therefore, considering the deviation of κ_c conversion and high sensitivity of AR_{sp} to κ_c when \ddot{A} is higher than 1.5, the method of calculating N_{CCN} from measurements of a humidified nephelometer system may lead to significant deviation in this case which means that this method can only be adopted when \ddot{A} is lower than 1.5.

Based on the lookup table of κ_c and \ddot{A} , AR_{sp} is calculated and applied to calculate N_{CCN} with σ_{sp} . The calculated AR_{sp} and N_{CCN} are compared with the measured AR_{sp} and N_{CCN} shown as the green dots in Figure 6. In general, good agreements between calculations and measurements are achieved and relative deviations are within 30%. For the comparison of AR_{sp} , the system relative deviation is less than 10%. For the comparison of N_{CCN} , the slope and the correlation coefficient of the regression are 1.03 and 0.966, respectively.

In addition, the influence of the κ_c conversion on AR_{sp} and N_{CCN} calculation are evaluated in two ways. In the first way, $\Delta\kappa$ of the κ_c conversion is set to be 0.05 higher or lower, which means $\Delta\kappa$ of 0.25 or 0.15. The corresponding results are presented as the red dots and blue dots in Figure 6. In the second way, a constant κ_c of 0.34, which is the average of κ_c values in Gucheng campaign, is used to calculate AR_{sp} and N_{CCN} , and shown as the grey dots in Figure 6. In general, differences among calculations using various κ_c conversions are quite small. The $\Delta\kappa$ difference of 0.05 in κ_c conversion only leads to a difference of 10% for the system relative deviation. The correlation coefficient of the calculation using a constant κ_c is just a little lower than correlation coefficients of calculations using a κ_c conversion. As a result, the method of calculating N_{CCN} is insensitive to the uncertainty of the κ_c conversion.

In this study, the insensitivity of calculated N_{CCN} to κ_c conversion is partly due to the small variation of κ_f during the campaign. On one hand, the variation of κ_c can be quite large and cause non-ignorable deviations of calculated N_{CCN} . As previous studies of N_{CCN} measurement showed, the variation of κ_c is often small and a constant κ_c can be used to calculate N_{CCN} accurately (Andreae and Rosenfeld, 2008; Gunthe et al., 2009; Rose et al., 2010; Deng et al., 2013). Results in this study are similar to these previous studies. However, large variations of κ_c are also found in some other

studies. In NCP, fluctuations of aerosol hygroscopicity during New Particle Formation events and soot emissions lead to significant deviations of calculated N_{CCN} from average aerosol hygroscopicity (Ma et al., 2016). On the other hand, the influence of κ_c cannot be ignored because the value of the average hygroscopicity is different in various regions during various periods. In summer of NCP, measured κ_f at sub-saturated conditions can reach up to 0.45 when inorganic compositions dominate in particles (Kuang et al., 2016). In this case, calculated N_{CCN} ignoring κ_c may be 10 times larger than measured N_{CCN} . To sum up, although the exact value of κ_c cannot be obtained from the measurement of the humidified nephelometer system, the influence of κ_c on N_{CCN} can be inferred and is found to be correct enough considering the convenience of this method. More data, especially in observations of more hygroscopic aerosol, is still needed to confirm this method.

4. Conclusions

N_{CCN} is a key parameter of cloud microphysics and aerosol indirect radiative effect. Direct measurements of N_{CCN} are generally conducted under super-saturated conditions in cloud chambers, and are complex and costly. The aerosols of accumulation mode contribute most to both the aerosol scattering coefficient and the aerosol CCN activity. In view of this, it is possible to predict N_{CCN} based on relationships between aerosol optical properties and the aerosol CCN activity. In this study, a new method is proposed to calculate N_{CCN} based on measurements of a humidified nephelometer system. In this method, N_{CCN} is derived from a look-up table which involves σ_{sp} , \tilde{A} and κ_f , and the required three parameters can be obtained from a three-wavelength humidified nephelometer system.

Relationships between aerosol optical properties and aerosol CCN activity are investigated using datasets about aerosol PNSD measured during several campaigns in the North China Plain. The relationship between σ_{sp} , \tilde{A} , κ_c and N_{CCN} is analyzed. It is found that the ratio between N_{CCN} and σ_{sp} , referred to as AR_{sp} , is determined by κ_c and \tilde{A} . In light of this, it is possible to calculate N_{CCN} based only on measurements of a three-wavelength humidified nephelometer system which provides information about σ_{sp} , the hygroscopicity parameter κ and \tilde{A} . —However, κ derived from measurements of a humidified nephelometer system under sub-saturated conditions (termed as κ_f)

differs from κ under super-saturated conditions which indicate CCN activity (termed as κ_c). As a result, the conversion from κ_f to κ_c is needed. Based on previous studies of aerosol hygroscopicity and CCN activity, a simple conversion from κ_f to κ_c with a fixed difference (referred to as $\Delta\kappa$) of 0.2 is proposed. On the basis of this simple conversion, the method of N_{CCN} prediction based only on measurements of a humidified nephelometer system is achieved under conditions without sea salt aerosol, ~~or dust aerosol~~, externally mixed aerosol or aerosol near single source regions.

This method is validated with measurements from a humidified nephelometer system and a CCN counter in Gucheng in 2016. During the campaign, both N_{CCN} and σ_{sp} vary with the pollution conditions. AR_{sp} is around 5 and changes with λ and κ_f . The difference between κ_f and κ_c , ~~was~~ 0.2 ± 0.1 . The agreement between the calculated N_{CCN} and the measured N_{CCN} is achieved with relative deviations less than 30%. Sensitivity of calculated N_{CCN} to conversions from κ_f to κ_c is studied by applying different kinds of conversions. Results show that calculated N_{CCN} varies little and is insensitive to the conversions, which confirms the robustness and applicability of this newly proposed method.

This study has connected aerosol optical properties with N_{CCN} , and also proposed a novel method to calculate N_{CCN} based only on measurements of a three-wavelength humidified nephelometer system. Due to the simple operation and stability of the humidified nephelometer system, this method will facilitate the real time monitoring of N_{CCN} , especially on aircrafts. In addition, measurements of the widely used CCN counter are limited to supersaturations higher than 0.07. This method is more suitable for calculating N_{CCN} at lower supersaturations, thus is more applicable for ambient measurements of clouds and fogs in the atmosphere.

Acknowledgement

This work is supported by the National Natural Science Foundation of China (41590872, 41375134 and 41505107).

Reference

- Andreae, M. O., and Rosenfeld, D.: Aerosol-cloud-precipitation interactions. Part 1. The nature and sources of cloud-active aerosols, *Earth-Science Reviews*, 89, 13-41, 10.1016/j.earscirev.2008.03.001, 2008.
- Andreae, M. O.: Correlation between cloud condensation nuclei concentration and aerosol optical thickness in remote and polluted regions, *Atmospheric Chemistry and Physics*, 9, 543-556, 2009.
- Brock, C. A., Wagner, N. L., Anderson, B. E., Attwood, A. R., Beyersdorf, A., Campuzano-Jost, P., Carlton, A. G., Day, D. A., Diskin, G. S., Gordon, T. D., Jimenez, J. L., Lack, D. A., Liao, J., Markovic, M. Z., Middlebrook, A. M., Ng, N. L., Perring, A. E., Richardson, M. S., Schwarz, J. P., Washenfelder, R. A., Welti, A., Xu, L., Ziemba, L. D., and Murphy, D. M.: Aerosol optical properties in the southeastern United States in summer – Part 1: Hygroscopic growth, *Atmos. Chem. Phys.*, 16, 4987-5007, 10.5194/acp-16-4987-2016, 2016.
- Chen, J., Zhao, C. S., Ma, N., and Yan, P.: Aerosol hygroscopicity parameter derived from the light scattering enhancement factor measurements in the North China Plain, *Atmos. Chem. Phys.*, 14, 8105-8118, 10.5194/acp-14-8105-2014, 2014.
- Cheng, Y. F., Wiedensohler, A., Eichler, H., Su, H., Gnauk, T., Brueggemann, E., Herrmann, H., Heintzenberg, J., Slanina, J., Tuch, T., Hu, M., and Zhang, Y. H.: Aerosol optical properties and related chemical apportionment at Xinken in Pearl River Delta of China, *Atmos. Environ.*, 42, 6351-6372, 10.1016/j.atmosenv.2008.02.034, 2008.
- Covert, D. S., Charlson, R., and Ahlquist, N.: A study of the relationship of chemical composition and humidity to light scattering by aerosols, *Journal of applied meteorology*, 11, 968-976, 1972.
- Cubison, M. J., Ervens, B., Feingold, G., Docherty, K. S., Ulbrich, I. M., Shields, L., Prather, K., Hering, S., and Jimenez, J. L.: The influence of chemical composition and mixing state of Los Angeles urban aerosol on CCN number and cloud properties, *Atmospheric Chemistry and Physics*, 8, 5649-5667, 2008.
- Deng, Z. Z., Zhao, C. S., Ma, N., Liu, P. F., Ran, L., Xu, W. Y., Chen, J., Liang, Z., Liang, S., Huang, M. Y., Ma, X. C., Zhang, Q., Quan, J. N., Yan, P., Henning, S., Mildenberger, K., Sommerhage, E., Schäfer, M., Stratmann, F., and Wiedensohler, A.: Size-resolved and bulk activation properties of aerosols in the North China Plain, *Atmos. Chem. Phys.*, 11, 3835-3846, 10.5194/acp-11-3835-2011, 2011.
- Deng, Z. Z., Zhao, C. S., Ma, N., Ran, L., Zhou, G. Q., Lu, D. R., and Zhou, X. J.: An examination of parameterizations for the CCN number concentration based on in situ measurements of aerosol activation properties in the North China Plain, *Atmos. Chem. Phys.*, 13, 6227-6237, 10.5194/acp-13-6227-2013, 2013.
- Dusek, U., Frank, G., Hildebrandt, L., Curtius, J., Schneider, J., Walter, S., Chand, D., Drewnick, F., Hings, S., and Jung, D.: Size matters more than chemistry for cloud-nucleating ability of aerosol particles, *Science*, 312, 1375-1378, 2006.
- Ervens, B., Cubison, M., Andrews, E., Feingold, G., Ogren, J. A., Jimenez, J. L., DeCarlo, P., and Nenes, A.: Prediction of cloud condensation nucleus number concentration using measurements of aerosol size distributions and composition and light scattering enhancement due to humidity, *Journal of Geophysical Research: Atmospheres*, 112, n/a-n/a, 10.1029/2006jd007426, 2007.
- Ervens, B., Cubison, M. J., Andrews, E., Feingold, G., Ogren, J. A., Jimenez, J. L., Quinn, P. K., Bates, T. S., Wang, J., Zhang, Q., Coe, H., Flynn, M., and Allan, J. D.: CCN predictions using simplified assumptions of organic aerosol composition and mixing state: a synthesis from six different locations, *Atmospheric Chemistry and Physics*, 10, 4795-4807, 10.5194/acp-10-4795-2010, 2010.
- Gasso, S., and Hegg, D. A.: On the retrieval of columnar aerosol mass and CCN concentration by MODIS, *J. Geophys. Res.-Atmos.*, 108, 4010, 10.1029/2002jd002382, 2003.
- Ghan, S. J., and Collins, D. R.: Use of in situ data to test a Raman lidar-based cloud condensation nuclei remote sensing method, *Journal of Atmospheric and Oceanic Technology*, 21, 387-394, 10.1175/1520-0426(2004)021<0387:uoisd>2.0.co;2, 2004.
- Ghan, S. J., Rissman, T. A., Elleman, R., Ferrare, R. A., Turner, D., Flynn, C., Wang, J., Ogren, J., Hudson, J., Jonsson, H. H., VanReken, T., Flagan, R. C., and Seinfeld, J. H.: Use of in situ cloud condensation nuclei, extinction, and aerosol size distribution measurements to test a method for retrieving cloud condensation nuclei profiles from surface measurements, *J. Geophys. Res.-Atmos.*, 111, D05s10, 10.1029/2004jd005752, 2006.
- Gunthe, S. S., King, S. M., Rose, D., Chen, Q., Roldin, P., Farmer, D. K., Jimenez, J. L., Artaxo, P., Andreae, M. O., Martin, S. T., and Poschl, U.: Cloud condensation nuclei in pristine tropical rainforest air of Amazonia: size-resolved measurements and modeling of

atmospheric aerosol composition and CCN activity, *Atmospheric Chemistry and Physics*, 9, 7551-7575, 2009.

Hudson, J. G.: AN INSTANTANEOUS CCN SPECTROMETER, *Journal of Atmospheric and Oceanic Technology*, 6, 1055-1065, 10.1175/1520-0426(1989)006<1055:aics>2.0.co;2, 1989.

Jefferson, A.: Empirical estimates of CCN from aerosol optical properties at four remote sites, *Atmos. Chem. Phys.*, 10, 6855-6861, 10.5194/acp-10-6855-2010, 2010.

Köhler, H.: The nucleus in and the growth of hygroscopic droplets, *Transactions of the Faraday Society*, 32, 1152-1161, 1936.

Kapustin, V. N., Clarke, A. D., Shinozuka, Y., Howell, S., Brekhovskikh, V., Nakajima, T., and Higurashi, A.: On the determination of a cloud condensation nuclei from satellite: Challenges and possibilities, *J. Geophys. Res.-Atmos.*, 111, D04202 10.1029/2004jd005527, 2006.

Kreidenweis, S. M., and Asa-Awuku, A.: 5.13 - Aerosol Hygroscopicity: Particle Water Content and Its Role in Atmospheric Processes A2 - Holland, Heinrich D, in: *Treatise on Geochemistry (Second Edition)*, edited by: Turekian, K. K., Elsevier, Oxford, 331-361, 2014.

Kuang, Y., Zhao, C. S., Ma, N., Liu, H. J., Bian, Y. X., Tao, J. C., and Hu, M.: Deliquescent phenomena of ambient aerosols on the North China Plain, *Geophys. Res. Lett.*, n/a-n/a, 10.1002/2016gl070273, 2016.

Kuang, Y., Zhao, C., Tao, J., Bian, Y., Ma, N., and Zhao, G.: A novel method to derive the aerosol hygroscopicity parameter based only on measurements from a humidified nephelometer system, *Atmos. Chem. Phys. Discuss.*, 2017, 1-25, 10.5194/acp-2016-1066, 2017a.

Kuang, Y., Zhao, C. S., Tao, J. C., Bian, Y. X., Ma, N., and Zhao, G.: A novel method for deriving the aerosol hygroscopicity parameter based only on measurements from a humidified nephelometer system, *Atmospheric Chemistry and Physics*, 17, 6651-6662, 10.5194/acp-17-6651-2017, 2017b.

Lance, S., Nenes, A., Medina, J., and Smith, J.: Mapping the operation of the DMT continuous flow CCN counter, *Aerosol science and technology*, 40, 242-254, 2006.

Lathem, T. L., and Nenes, A.: Water Vapor Depletion in the DMT Continuous-Flow CCN Chamber: Effects on Supersaturation and Droplet Growth, *Aerosol science and technology*, 45, 604-615, 10.1080/02786826.2010.551146, 2011.

Liu, H. J., Zhao, C. S., Nekat, B., Ma, N., Wiedensohler, A., van Pinxteren, D., Spindler, G., Müller, K., and Herrmann, H.: Aerosol hygroscopicity derived from size-segregated chemical composition and its parameterization in the North China Plain, *Atmos. Chem. Phys.*, 14, 2525-2539, 10.5194/acp-14-2525-2014, 2014.

Liu, J. J., and Li, Z. Q.: Estimation of cloud condensation nuclei concentration from aerosol optical quantities: influential factors and uncertainties, *Atmospheric Chemistry and Physics*, 14, 471-483, 10.5194/acp-14-471-2014, 2014.

Ma, N., Zhao, C., Nowak, A., Müller, T., Pfeifer, S., Cheng, Y., Deng, Z., Liu, P., Xu, W., and Ran, L.: Aerosol optical properties in the North China Plain during HaChi campaign: an in-situ optical closure study, *Atmos. Chem. Phys.*, 11, 5959-5973, 2011.

Ma, N., Zhao, C., Tao, J., Wu, Z., Kecorius, S., Wang, Z., Größ, J., Liu, H., Bian, Y., Kuang, Y., Teich, M., Spindler, G., Müller, K., van Pinxteren, D., Herrmann, H., Hu, M., and Wiedensohler, A.: Variation of CCN activity during new particle formation events in the North China Plain, *Atmos. Chem. Phys.*, 16, 8593-8607, 10.5194/acp-16-8593-2016, 2016.

McMeeking, G. R., Morgan, W. T., Flynn, M., Highwood, E. J., Turnbull, K., Haywood, J., and Coe, H.: Black carbon aerosol mixing state, organic aerosols and aerosol optical properties over the United Kingdom, *Atmos. Chem. Phys.*, 11, 9037-9052, 10.5194/acp-11-9037-2011, 2011.

Moteki, N., and Kondo, Y.: Effects of Mixing State on Black Carbon Measurements by Laser-Induced Incandescence, *Aerosol science and technology*, 41, 398-417, 10.1080/02786820701199728, 2007.

Nenes, A., Chuang, P. Y., Flagan, R. C., and Seinfeld, J. H.: A theoretical analysis of cloud condensation nucleus (CCN) instruments, *J. Geophys. Res.-Atmos.*, 106, 3449-3474, 10.1029/2000jd900614, 2001.

Petters, M. D., and Kreidenweis, S. M.: A single parameter representation of hygroscopic growth and cloud condensation nucleus activity, *Atmospheric Chemistry and Physics*, 7, 1961-1971, 2007.

Roberts, G., and Nenes, A.: A continuous-flow streamwise thermal-gradient CCN chamber for atmospheric measurements, *Aerosol science and technology*, 39, 206-221, 2005.

Rose, D., Gunthe, S., Mikhailov, E., Frank, G., Dusek, U., Andreae, M., and Pöschl, U.: Calibration and measurement uncertainties of a

continuous-flow cloud condensation nuclei counter (DMT-CCNC): CCN activation of ammonium sulfate and sodium chloride aerosol particles in theory and experiment, *Atmospheric Chemistry and Physics*, 8, 1153-1179, 2008.

Rose, D., Nowak, A., Achtert, P., Wiedensohler, A., Hu, M., Shao, M., Zhang, Y., Andreae, M. O., and Poschl, U.: Cloud condensation nuclei in polluted air and biomass burning smoke near the mega-city Guangzhou, China - Part 1: Size-resolved measurements and implications for the modeling of aerosol particle hygroscopicity and CCN activity, *Atmospheric Chemistry and Physics*, 10, 3365-3383, 2010.

Shinozuka, Y., Clarke, A. D., Nenes, A., Jefferson, A., Wood, R., McNaughton, C. S., Ström, J., Tunved, P., Redemann, J., Thornhill, K. L., Moore, R. H., Latham, T. L., Lin, J. J., and Yoon, Y. J.: The relationship between cloud condensation nuclei (CCN) concentration and light extinction of dried particles: indications of underlying aerosol processes and implications for satellite-based CCN estimates, *Atmos. Chem. Phys.*, 15, 7585-7604, 10.5194/acp-15-7585-2015, 2015.

Titos, G., Cazorla, A., Zieger, P., Andrews, E., Lyamani, H., Granados-Muñoz, M. J., Olmo, F. J., and Alados-Arboledas, L.: Effect of hygroscopic growth on the aerosol light-scattering coefficient: A review of measurements, techniques and error sources, *Atmos. Environ.*, 141, 494-507, <http://dx.doi.org/10.1016/j.atmosenv.2016.07.021>, 2016.

Wex, H., McFiggans, G., Henning, S., and Stratmann, F.: Influence of the external mixing state of atmospheric aerosol on derived CCN number concentrations, *Geophys. Res. Lett.*, 37, L10805 10.1029/2010gl043337, 2010.

Whitehead, J. D., Irwin, M., Allan, J. D., Good, N., and McFiggans, G.: A meta-analysis of particle water uptake reconciliation studies, *Atmos. Chem. Phys.*, 14, 11833-11841, 10.5194/acp-14-11833-2014, 2014.

Wu, Z. J., Poulain, L., Henning, S., Dieckmann, K., Birmili, W., Merkel, M., van Pinxteren, D., Spindler, G., Mueller, K., Stratmann, F., Herrmann, H., and Wiedensohler, A.: Relating particle hygroscopicity and CCN activity to chemical composition during the HCCT-2010 field campaign, *Atmospheric Chemistry and Physics*, 13, 7983-7996, 10.5194/acp-13-7983-2013, 2013.

Renbaum-Wolff, L., M. Song, et al. (2016). "Observations and implications of liquid-liquid phase separation at high relative humidities in secondary organic material produced by α -pinene ozonolysis without inorganic salts." *Atmos. Chem. Phys.* **16**(12): 7969-7979.

Irwin, M., N. Good, et al. (2010). "Reconciliation of measurements of hygroscopic growth and critical supersaturation of aerosol particles in central Germany." *Atmos. Chem. Phys.* **10**(23): 11737-11752.

Good, N., D. O. Topping, et al. (2010). "Consistency between parameterisations of aerosol hygroscopicity and CCN activity during the RHaMBLe discovery cruise." *Atmospheric Chemistry and Physics* **10**(7): 3189-3203.

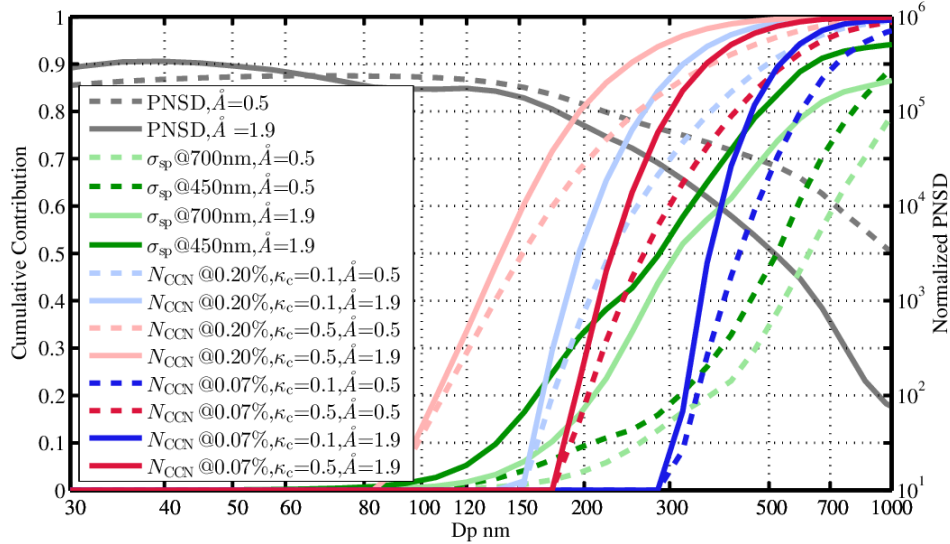
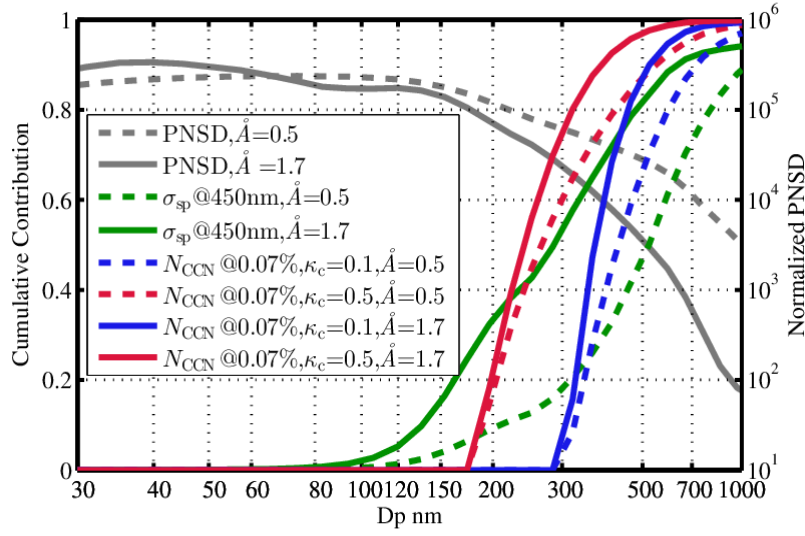


Figure 1.

Aerosol PNSD (black lines), the cumulative contribution of σ_{sp} at wavelength of 450nm and 700nm (dark green lines and light green lines, respectively), and the cumulative contribution of N_{CCN} at supersaturation of 0.07% (dark red and dark blue lines) and the cumulative contribution of N_{CCN} at supersaturation of 0.20% (light red and light blue lines) based on measurement in several campaigns in the North China Plain. Solid lines and dashed lines indicate \bar{A} of 1.7 and 0.5, respectively. Blue lines and red lines indicate κ_c of 0.1 and 0.5, respectively.

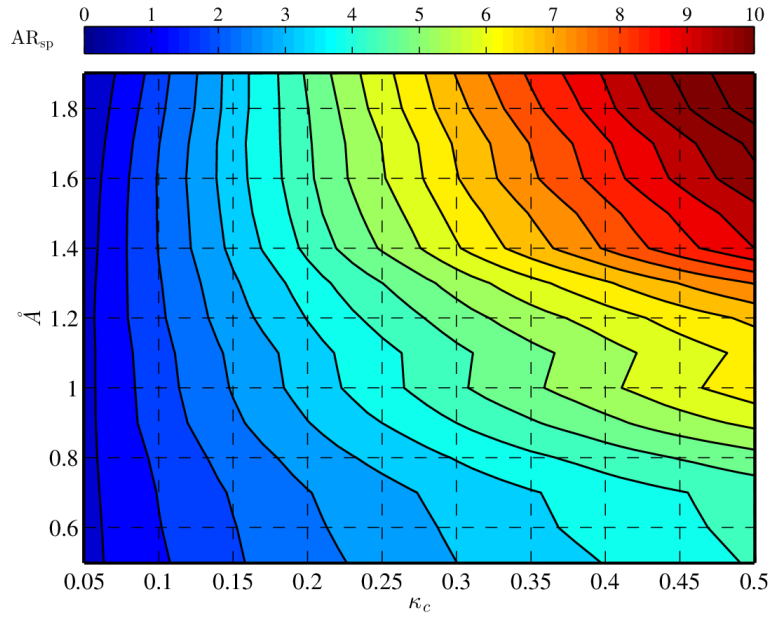
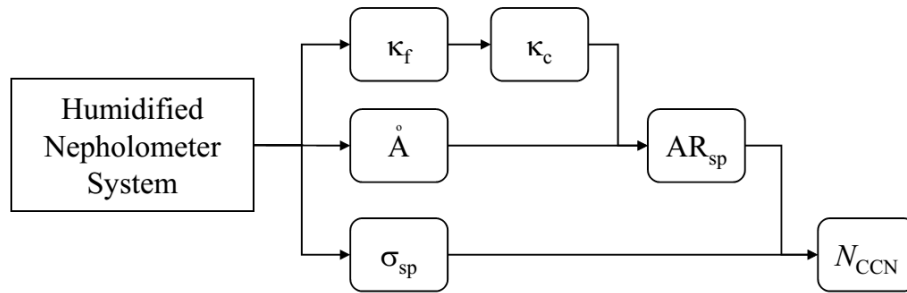


Figure 2.

Colors represent AR_{sp} (calculated as $AR_{sp} = \frac{N_{CCN}}{\sigma_{sp}}$ at 450nm wavelength and 0.07% supersaturation) with different PNSDs (classified by \dot{A} values) and different κ_c . Colors represent AR_{sp} (ratios between N_{CCN} and σ_{sp}) with κ_c and \dot{A} .



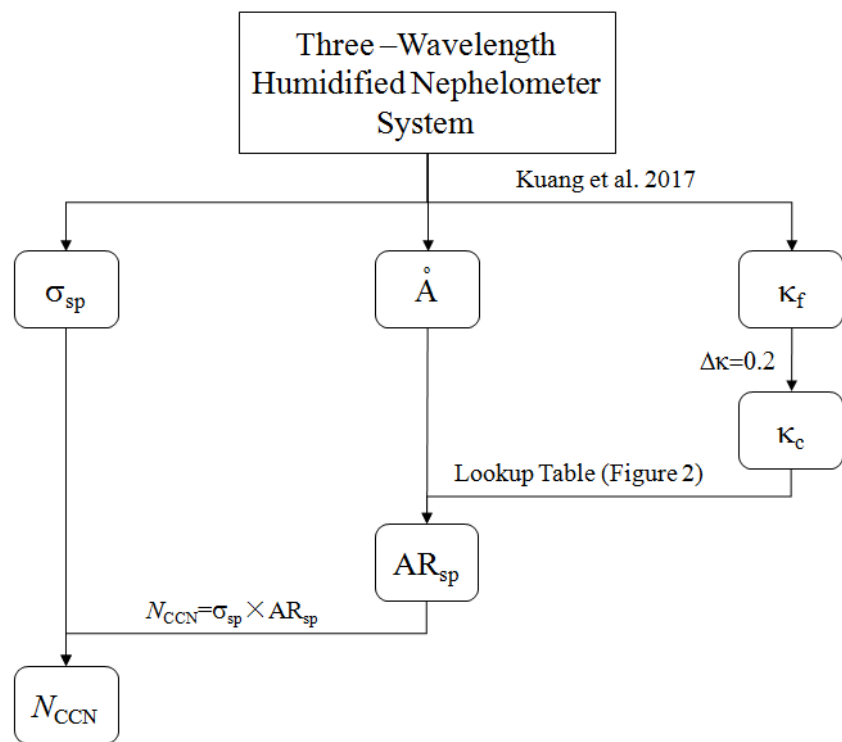


Figure 3.

The schematic chart of the N_{CCN} prediction based on measurements of a humidified nephelometer system.

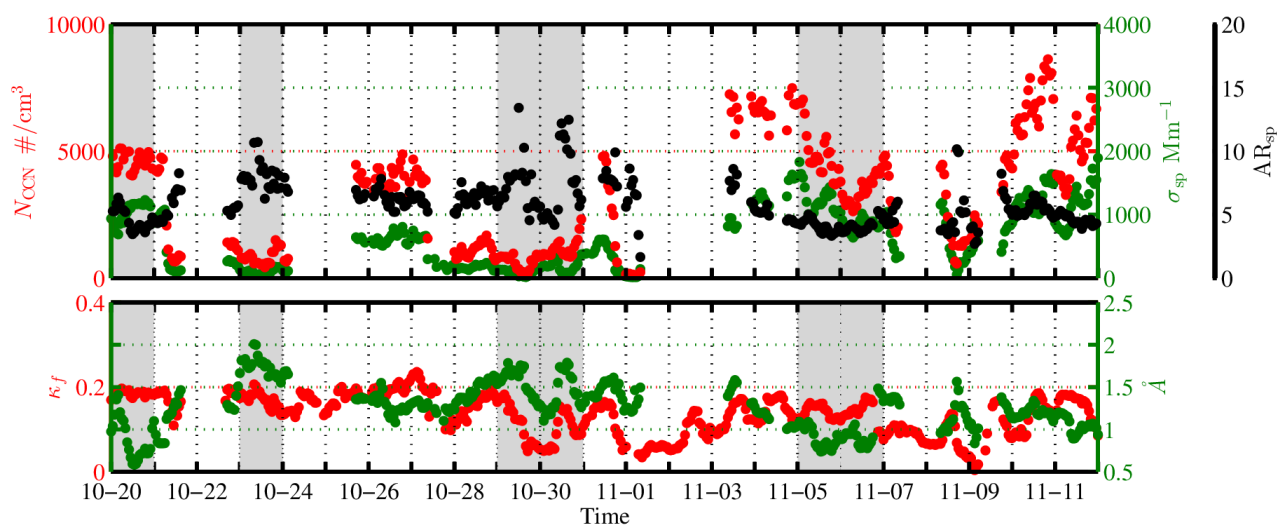


Figure 4.

Overview of measurements in Gucheng in 2016. Upper plot: time series of N_{CCN} at the supersaturation of 0.07% (red dots), σ_{sp} at the wavelength of 50nm (green dots) and their ratios

(black dots), referred to as AR_{sp} . Lower plot: time series of κ_f (red dots) and \ddot{A} (green dots). The grey bars are periods when the sensitivity of AR_{sp} to κ_c is notable.

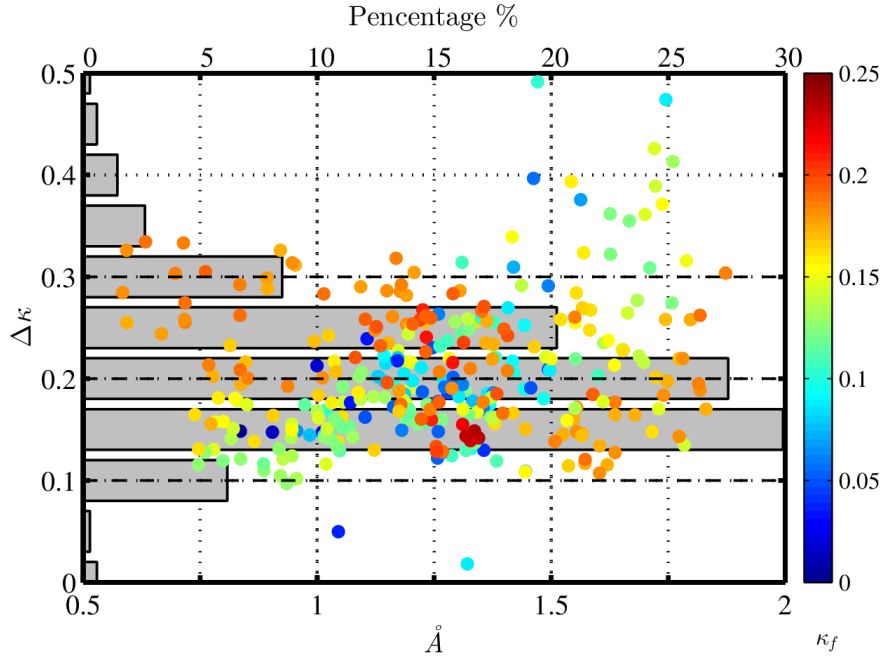
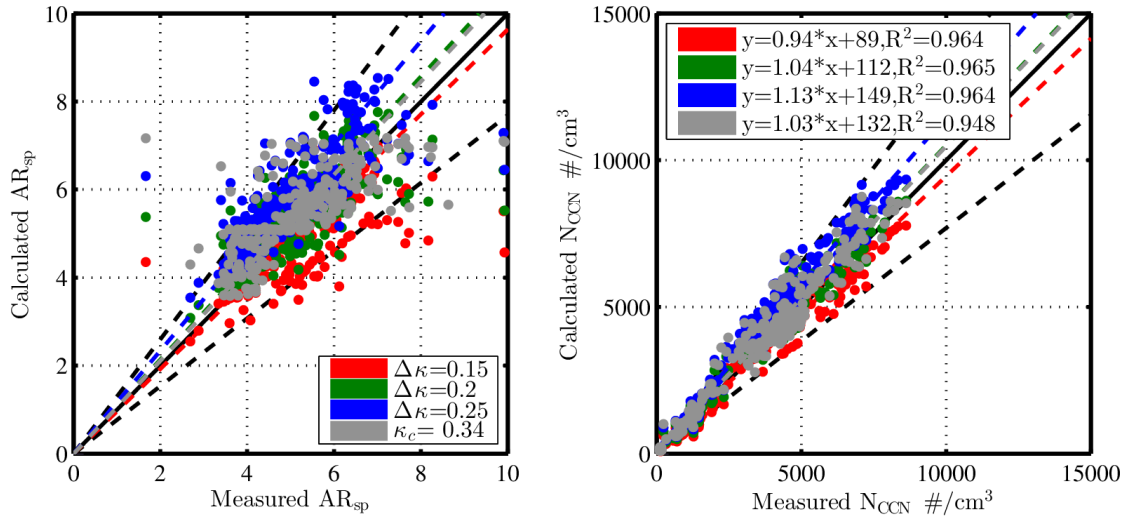


Figure 5.

Differences between κ_c and κ_f , referred to as $\Delta\kappa$, with \ddot{A} (positions of dots) and κ_f (colors of dots). Bars represent percentages of $\Delta\kappa$ within different ranges.



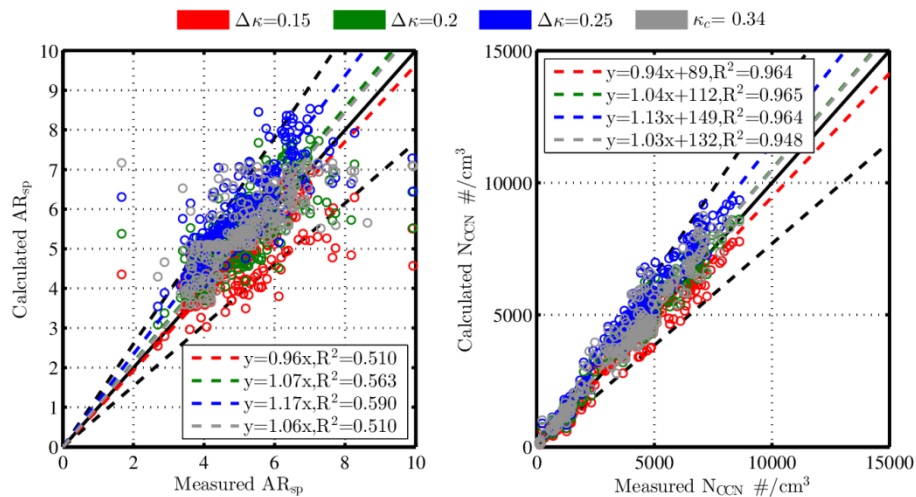


Figure 6.

Left plot: comparisons of calculated AR_{sp} and measured AR_{sp} with different conversions of κ_c from κ_f . Right plot: regressions of calculated N_{CCN} and measured N_{CCN} with different conversions of κ_c from κ_f .

Campaign	Air mass	Parameter	Caveats	Results	Reference
ICARTT ¹ in the north eastern USA and Canada	Polluted air mass	fRH and PNSD	Calculate N_{CCN} with aerosol hygroscopicity constrained by f(RH) and PNSD.	Predict N_{CCN} at SS > 0.3% with a 0.9 R^2 .	Ervens et al., 2007
HaChi ² on the North China Plain	Aged continental air mass	PNSD and fRH	Similar to Ervens et al., 2007. Calculate N_{CCN} with the hygroscopicity parameter constrained by f(RH) and PNSD.	Slopes around 1 and R^2 around 0.9.	Chen et al., 2014
TARFOX ³ Atlantic seaboard and ACE-2 ⁴	Polluted air mass	Retrieved aerosol volume from remote sensing	Predict N_{CCN} from aerosol volumes with empirical number-to-volume concentration ratio	Overestimate up to 5 times	Gasso and Hegg, 2003

<u>ACE-2 in northeastern Atlantic</u>	<u>Diverse air mass</u>	<u>Backscatter or extinction profile. CCN at the surface.</u>	<u>Retrieve N_{CCN} profile from backscatter (or extinction) vertical profile assuming their ratios are the same to the ratio at surface, which can be calculated by backscatter (or extinction) and N_{CCN} measured at the surface</u>	<u>Predict N_{CCN} on most days for 0.1% SS and on 20%–40% of the days at 1% SS.</u>	<u>Ghan and Collins, 2004</u>
<u>ARM⁵ Climate Research Facility central site at the Southern Great Plains</u>	<u>Continental air mass</u>	<u>Backscatter (or extinction) and RH profile. fRH and CCN at surface</u>	<u>Same as Ghan and Collins, 2004.</u>	<u>Explains CCN variance for 25%–63% of all measurements at high supersaturations</u>	<u>Ghan et al., 2006</u>
<u>TRACE-P⁶ and ACE-Asia⁷</u>	<u>Asian outflow over the western Pacific</u>	<u>Aerosol Index (AI, the product of ambient light extinction and \dot{A})</u>	<u>Predict N_{CCN} based on empirical relationship between AI and N_{CCN}</u>	<u>AI relate well to CCN only with suitably stratified data</u>	<u>Kapustin et al., 2006</u>
<u>Multiple measurements</u>	<u>Diverse air mass</u>	<u>AERONET aerosol optical thickness (AOT)</u>	<u>Predict N_{CCN} based on empirical relationship between AOT and N_{CCN} as a power law</u>	<u>Predict N_{CCN} at SS > 0.3% with a 0.88 R^2, but have a factor-of-four range of N_{CCN} at a given AOT</u>	<u>Andreae, 2009</u>
<u>Four ARM sites</u>	<u>Polluted air mass</u>	<u>SSA, backscatter fraction and σ_{sp}</u>	<u>Estimate N_{CCN} from fitting parameters for the N_{CCN} activity spectra, which can be calculate based on their empirical relationships with aerosol optical properties.</u>	<u>Predict N_{CCN} with slopes around 0.9 and R^2 around 0.6.</u>	<u>Jefferson, 2010</u>
<u>Multiple ARM sites around the world</u>	<u>Diverse air mass</u>	<u>RH, fRH, SSA, AOT and σ_{sp}</u>	<u>Calculate N_{CCN} with σ_{sp} (or AOT) based on their empirical relationship, whose impact RH, fRH and SSA.</u>	<u>Achieve the best results by using σ_{sp} and SSA. Weakly affect on the σ_{sp}–N_{CCN}</u>	<u>Liu and Li, 2014</u>

				<u>relationship by fRH.</u>	
				<u>Deteriorate</u>	
				<u>N_{CCN}-AOT</u>	
				<u>relationship with</u>	
				<u>increasing RH</u>	
	<u>Multiple</u>	<u>Diverse air</u>	<u>\tilde{A} and</u>	<u>Calculate N_{CCN} with light</u>	<u>Shinozuka</u>
	<u>ARM sites</u>	<u>mass not</u>	<u>extinction</u>	<u>extinction based on their</u>	<u>et al.,</u>
	<u>around the</u>	<u>dominated</u>	<u>coefficient</u>	<u>emperical relationship.</u>	<u>2015</u>
	<u>world</u>	<u>by dust</u>			
529	<u>Tabel 1.</u>				
530	<u>Review of studies that have used aerosol optical parameters to infer N_{CCN}.</u>				
531	<u>¹ International Consortium for Atmospheric Research on Transport and Transformation.</u>				
532	<u>² Haze in China.</u>				
533	<u>³ Troposphere Aerosol Radiative Forcing Experiment.</u>				
534	<u>⁴ Second Aerosol Characterization Experiment.</u>				
535	<u>⁵ Atmospheric Radiation Measurement.</u>				
536	<u>⁶ Transport and Chemical Evolution over the Pacific.</u>				
537	<u>⁷ Aerosol Characterization Experiment-Asia.</u>				
538					